Available online at www.sciencedirect.com
ScienceDirect
Journal of the European Ceramic Society 31 (2011) 3081–3086
www.elsevier.com/locate/jeurceramsoc

Long-term degradation of Ta_2O_5-doped Bi_2O_3 systems

S.E. Lin, W.C.J. Wei *

Dept. Mat. Sci. Eng., National Taiwan University, 1 Roosevelt Rd., Sect. 4, Taipei 106, Taiwan, ROC

Available online 14 May 2011

Abstract

Bismuth oxide in δ-phase is a well-known high oxygen ion conductor and can be used as an electrolyte for intermediate temperature solid oxide fuel cells (IT-SOFCs). 5–10 mol% Ta_2O_5 are doped into Bi_2O_3 to stabilize δ-phase by solid state reaction process. One Bi_2O_3 sample (7.5TSB) was stabilized by 7.5 mol% Ta_2O_5 and exhibited single phase δ-Bi_2O_3-like (type I) phase. Thermo-mechanical analyzer (TMA), X-ray diffractometry (XRD), AC impedance and high-resolution transmission electron microscopy (HRTEM) were used to characterize the properties. The results showed that holding at 800–850 °C for 1 h was the appropriate sintering conditions to get dense samples. Obvious conductivity degradation phenomenon was obtained by 1000 h long-term treatment at 650 °C due to the formation of α-Bi_2O_3 phase and Bi_3TaO_7, and ⟨1 1 1⟩ vacancy ordering in Bi_3TaO_7 structure.

Keywords: Ta_2O_5; Bi_2O_3; Fuel cell; Annealing; Conductivity

1. Introduction

Bismuth oxide (Bi_2O_3) was considered to be a potential ceramic material used as an electrolyte in intermediate temperature solid oxide fuel cells (IT-SOFCs) because of its high symmetric fluorite structure and high percentage of oxygen vacancies.[1] In the past century, numbers of the investigation results have been published and discussed on phase transition and related ionic conductivity of the polymorphism of pure and doped-Bi_2O_3.[2–4] In summary, at room temperature, the monoclinic α-phase is the stable phase. During heating, it transforms to fcc δ-phase at about 730 °C, which is stable up to its melting point at 825 °C. When cooling, a large thermal hysteresis occurs. Two possible intermediate metastable phases may appear, either a tetragonal β-phase at 650 °C or a γ-phase in bcc structure at 640 °C. The α-, β-, and γ-phases exhibit relatively low ionic conductivity, whereas the δ-phase performs very high ionic conductivity, two orders of magnitude higher than that of yttria-stabilized zirconia (YSZ).

The main problem for the use of δ-Bi_2O_3 is the thermal stability, which allows the use of this material only between 725 °C and 825 °C. The preservation of Bi_2O_3 in the fluorite structure to lower temperatures is of great interest, particularly to recent development of IT-SOFC. Many researchers have reported their efforts on how to stabilize the cubic phase to low temperature, mainly by substitution with alkaline and/or rare-earth elements. One well-known system is Bi_2O_3–VO_x ($BiMeVO_x$), where Me is an oxide dopant. The structure might transform to $BiVO_4$, which is one of bismuth vanadates.[5] Additionally, in some cases high valence elements as dopants for stabilizing the cubic structure are used, i.e. [Mo^{6+}],[4,6,7] [W^{6+}],[8,9] [Ta^{5+}],[4,8,10–13] [P^{5+}],[9] [Nb^{5+}],[4,8] [Sn^{4+}],[14] [Zr^{4+}],[8,15,16] [Ti^{4+}],[17] which results in the loss of oxygen vacancy.

Ta_2O_5-stabilized Bi_2O_3 (TSB) systems in a wide Ta-doping ratio, from 1.64 mol% to 50 mol%, have been well studied[4,10,12] concerning their crystal structure aspect. Several phases or intermediate compounds were identified, including

(1) β (tetragonal) structure, in the range of 1–4% TSB;
(2) type I structure (fluorite-like cubic structure) with 2 × 2 × 2 superstructure derived form δ-Bi_2O_3, normally found in the range of 5–10% TSB;
(3) type II structure (fluorite-like cubic structure) with 8 × 8 × 8 supercell based on δ-Bi_2O_3, normally found in the range of 10–25% TSB;
(4) type II* structure with distorted fluorite-like or pyrochlore-like Ta_4O_{18} tetrahedral clusters in the main structure, normally found around 30TSB;
(5) type III structure in monoclinic symmetry and a composition of 33.3% TSB, which is not a stable phase, but exists

* Corresponding author. Tel.: +886 2 33661317; fax: +886 2 363 4562.
E-mail address: wjwei@ntu.edu.tw (W.C.J. Wei).

0955-2219/$ – see front matter © 2011 Elsevier Ltd. All rights reserved.
doi:10.1016/j.jeurceramsoc.2011.04.015

between type II* and IV, if treated at high temperature, e.g., 1000 °C for 24 h;

(6) type IV structure in monoclinic symmetry and a composition of 35% TSB. The structure shows a stepped superstructure belonging to one of Aurivillius families.

Additionally, the superior conductivity results, i.e. greater than 10^{-1} S/cm at or below 650 °C, in the range of 3–12 mol% Ta_2O_5 dopant concentration (as abbreviated as 3TSB to 12TSB), have also been reported and are acceptable for IT-SOFC.[11,12] If the Ta concentration is less than 5 mol%, the sample shows two-step conduction mechanism because of its phase transformation.[12] Furthermore, the conductivity decreases with the increasing Ta doping amount accordingly.[12] The suitable doping level of Ta_2O_5 should be controlled in this region to prevent the formation of a second phase and stabilized to maintain δ-like phase to temperatures lower than 650 °C.

In the present work, three samples (5TSB, 7.5TSB and 10TSB) have been selected as the study subjects. We conducted long-term stability tests at 650 °C, which is the main issue to discuss and report.

2. Experiment procedure

Reagent grade starting powders, Bi_2O_3 (>99%, Solartech, Taiwan) and Ta_2O_5 (>99%, SIGMA Lot 61H3532) with size distributions of 1–2 μm and 0.2–0.5 μm, respectively, were prepared according to the composition of 5, 7.5 and 10 mol% Ta_2O_5 doped Bi_2O_3 (5TSB, 7.5TSB and 10TSB).The two starting oxides were dispersed separately in de-ionized water with 1 wt% ammonium salt homopolymer with a 2-propenoic acid group (D-134, Dai-Ichi Kogyo Seiyaku Co., Ltd., Japan) as dispersant and with 2 mm ZrO_2 balls as the milling media in a turbo-mixer. After milling for 24 h, the two slurries were mixed together for additional 4 h milling. The well mixed slurries were dried by a rotary vacuum evaporator (EYELA, Japan). Thereafter, 1.5 g dried mixture was die-pressed to disk. The detail processing steps are similar as reported in a previous publication.[18] All the samples in this study were sintered and cooled in a furnace without "quenching" step, which was used in the cases reported by others.[4,12]

As-polished and fractured surfaces of the sintered samples were investigated by field-emission-gun scanning electron microscope (FEG-SEM, LEO Instrument, Cambridge, UK) equipped with X-ray energy dispersive spectroscopy (EDS, DX-4, EDAZ Co., USA). The crystalline phases were also investigated by X-ray diffractometry (XRD, X' Pert Pro, PANalytical Co., Netherlands) with Cu Kα radiation, and analytical transmission electron microscopy (TEM, Tecnai F20, Philips Co., The Netherlands). Sintering behavior of the samples was characterized by thermal mechanical analysis (TMA, Setsys TMA 16/18, Setaram Co., France).

Real-time phase transformation of the samples was characterized by high temperature XRD (Rigaku TTRAX 3, Japan) to differentiate the effects of heating rate and holding time. The samples for high temperature XRD test were in powder state.

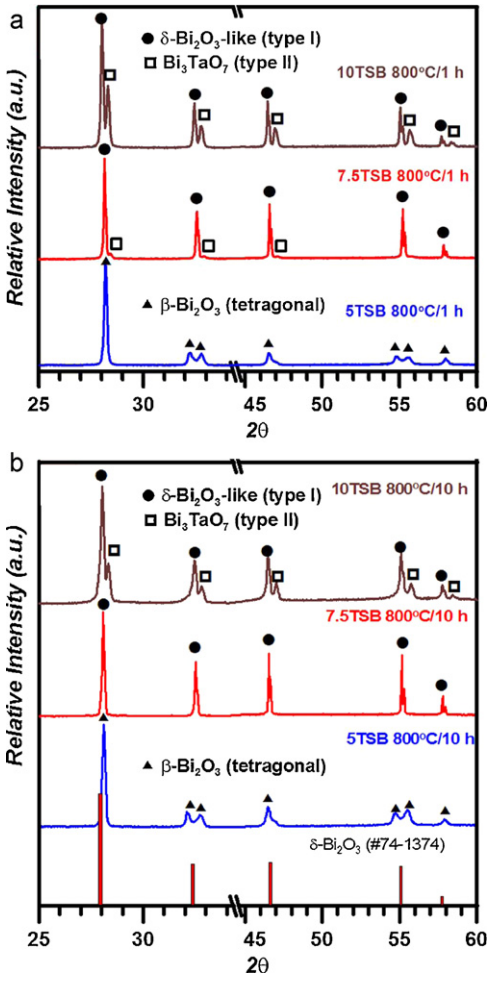

Fig. 1. XRD patterns of 5TSB, 7.5TSB and 10TSB annealed at 800 °C for (a) 1 and (b) 10 h. The line markers located on the bottom of (b) represent the diffraction intensity of pure δ-Bi_2O_3 phase (JCPD#74-1374).

Electrochemical characterization was performed on symmetric cell configuration. Ag paste electrodes were painted onto each surface of sintered disk and calcined at 400 °C for 30 min. Electrochemical impedance spectroscopy (EIS) measurement was executed in the temperature range of 400–650 °C by a potentiostat (Reference 30000, Gamry Instruments, Inc., US) in the frequency range 10 mHz–10^6 Hz. The heating rate was 10 °C/min and holding for 10 min at each 50 °C interval. An inductance loop in the impedance plots was subtracted to obtain the corrected impedance spectra. Conductivity is calculated from the value of bulk resistance, which is obtained from the intercept of the impedance spectra with the Z' axis.

3. Results and discussion

Fig. 1(a) shows the room temperature powder XRD patterns for 5TSB, 7.5TSB and 10TSB, annealed at 800 °C for 1 h (slowly cooled in air furnace). Two phases, δ-Bi_2O_3 (type I)[10] and Bi_3TaO_7 (type II)[10] can be observed in the pattern of 10TSB, which is identical to Zhou's[10] and Saito's[12] reports. Additionally, no Ta_2O_5 phases are indexed. Type I and type II structures show the different space groups $Pn\bar{3}m$ (2 2 5) and

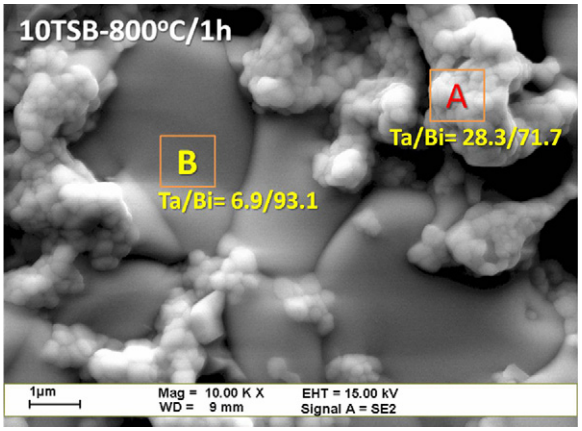

Fig. 2. SEM micrograph of as-fired 10TSB sintered at 800 °C for 1 h.

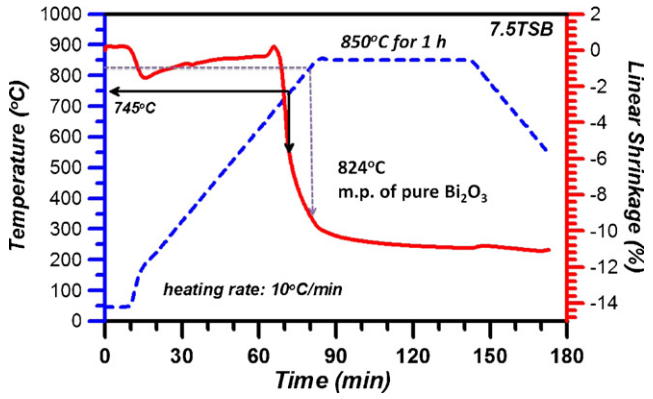

Fig. 3. TMA test of 7.5TSB sample, revealing the temperatures 745–800 °C to be the appropriate sintering temperature.

$Fm\bar{3}m$ (2 2 4), and lattice parameters 5,47.1 pm and 5,52.5 pm, respectively. Therefore, the 2θ difference of the strongest peak (1 1 1) for type I and type II is approximately 0.3° (27.948° and 28.227° for type I and type II, respectively). The tiny intensity of type II phase is still differentiable in the XRD pattern of 7.5TSB, indicating that the sample is not pure yet.

Fig. 1(b) reveals the three cases annealed for 10 h, where the pattern of 7.5TSB shows only type I structure, implying that the solid solution limit of Ta_2O_5 in Bi_2O_3 structure is less than 10 mol%. As the doping amount was 5 mol%, tetragonal β-type phase appeared. If the doping level is less than 4.5 mol%, a distorted tetragonal structure would be formed.[12] Zhou[10] reported that two phases, type I and β-Bi_2O_3, can co-exist if the Ta_2O_5 doping level is less than 4 mol% and higher than 2.5 mol%.

The needed amount of Ta_2O_5 to stabilize cubic δ-Bi_2O_3 is between 5% and 10%. This stabilization region is similar to that of yttria stabilized zirconia (YSZ) system, if the doping amount of Y_2O_3 decreases from 8 mol% (8YSZ) to 3 mol% (3YSZ),[19] the phase changed from cubic to tetragonal. The pattern of 7TSB reported by Saito and Midda[12] was indexed as cubic structure with a slightly large cell parameter of $a = 5{,}53.1$ pm.

Fig. 2 shows SEM as fired surface image of 800 °C/1 h sintered 10TSB. Two distinct features can be observed, fine grains in bright contrast and large grains in dark contrast. SEM-EDS in semi-quantitative analysis revealed that Ta/Bi ratio was 28.3/71.7 or 6.9/93.1 at regions A and B, respectively. Comparing with XRD results in Fig. 1, the bright small grains could be the type II phase and darker grains with larger grain size are type I phase. XRD result (not shown here) of 10TSB calcined at 800 °C for 10 h, then ground to powder and sintered at 850 °C for 20 h, two phases were obtained as expected.

Thermo-mechanical analysis were carried out in order to get a fully dense single phase TSB sample. Fig. 3 shows the fast shrinkage point located at 745 °C and kept sintering until to 850 °C. Therefore, 850 °C is an appropriated temperature to sinter 7.5TSB system. 96.5% theoretical density (T.D.) sample can be obtained through this process.

SEM micrographs of as-polished surfaces and cross sectional microstructures of 850 °C/1 h sintered 7.5TSB samples are shown in Fig. 4. Large grain size, around 20 μm can be observed at low magnification (Fig. 4(a-1)). The sample is fully dense, no pores are noted. Several small triangular precipitates (~200 nm) were observed in the enlarged image (Fig. 4(a-2)). However, no precipitates were found in the cross sectional image (Fig. 4(b-2)), implying these small precipitates only exist on the surface of the sample. SEM-EDS cannot distinguish the compositional difference between the precipitate and matrix phases because the size of the precipitates is too small to identify. This precipitates can be observed in 5TSB in this study and 5 mol% Sb_2O_3-doped Bi_2O_3 system reported by Fruth et al.[11]

TEM investigation of the sintered 7.5TSB sample is shown in Fig. 5. The small precipitates observed in SEM image (Fig. 4(a-2)) are not found in the TEM, except nano-pores and other interesting crystalline information. The high-resolution TEM image reveals that nano-pores, about 5 nm in diameter exist in the grain. The diffraction pattern confirms that the grain is type I (or cubic-fluorite structure) showing a super-lattice (as corresponding pattern pointed by arrows in Fig. 5(b)) with the diffraction along the ⟨1 0 0⟩ direction, implying long-range ordering of oxygen sublattice (in other words, the ordering of oxygen ions and vacancies). Both features, ordering of oxygen vacancies and formation of nano-pores contribute to the decrease of electric conductivity.

The results of EIS measurements and electrical properties of sintered 7.5TSB are shown in Figs. 6 and 7. Fig. 6 shows the Nyquist plots of the sample varied with testing temperatures. A Warberg-type impedance, which is apparent at low-frequency range,[20] can be observed at 400 °C, implying gas diffusion at electrodes. The bulk resistance of 7.5TSB decreased with the increase of the temperature. After normalization of electrode area and thickness of the sample, the conductivity of 7.5TSB is 0.31 (or $10^{-0.5}$) S/cm at 650 °C, which is comparable with the conductivity of 7TSB reported by Saito and Miida.[12]

The conductivity change of the sintered 7.5TSB is shown in Fig. 7 as a function of the annealing time at 650 °C. The bulk and interface resistances increase with the annealing time. The increase of bulk resistance may be attributed by the formation of new phases.

A decrease in the conductivity, 10% lower than the original value, was noted after annealed for 40 h. Similar phenomena of conductivity degradation are also observed in several

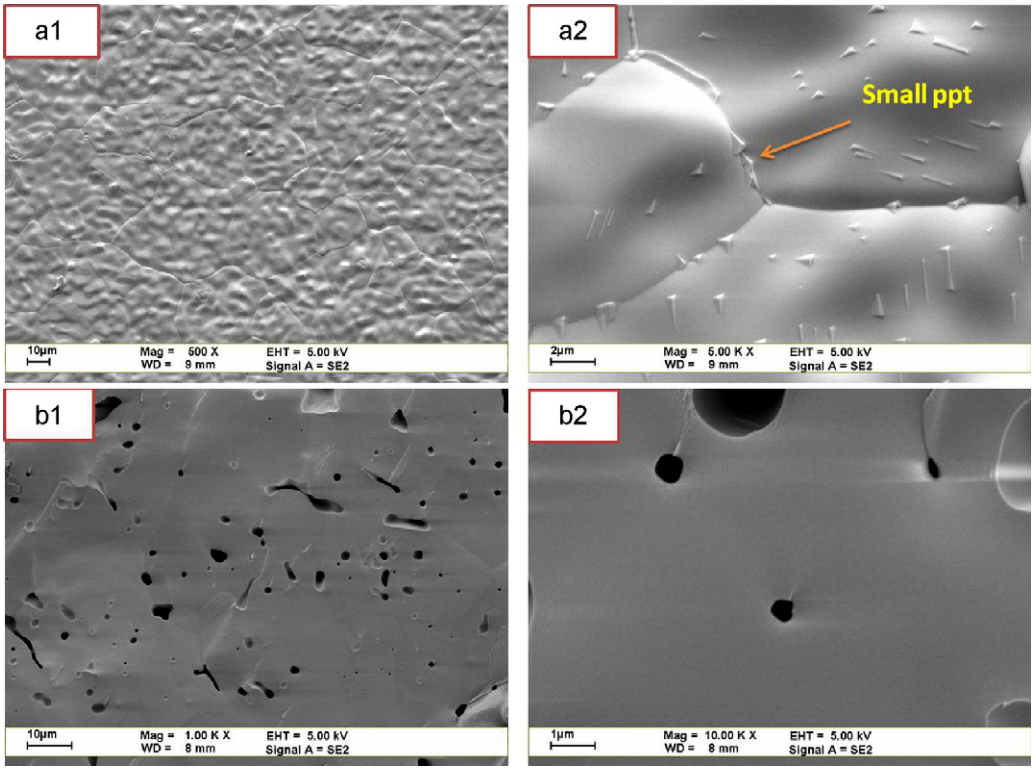

Fig. 4. SEM micrographs of 850 °C/1 h sintered 7.5TSB. (a-1) and (a-2) As-fired surfaces, (b-1) and (b-2) fracture surfaces, which are next to the as-fired surface in (a).

cases, for instance, 5TSB case reported by Saito and Midda,[12] and in Bi_2O_3–Er_2O_3 (or Gd_2O_3),[16] Bi_2O_3–Er_2O_3–PbO[20] or Bi_2O_3–M_2O_3 (M represents rare earth elements).[21] Fung et al.[16] considered the degradation in conductivity resulted from cubic to rhombohedral transformation, and proposed that could be suppressed by the addition of ZrO_2. This thermodynamic phase change for Bi_2O_3-based materials is one of few disadvantages for the application as SOFC electrolyte. Jiang and Wachsman[21] regarded the time-dependent conductivity decay was due to order (fcc-rhombohedral)–disorder (relaxed fcc-rhombohedral) transition for cubic "phase-stabilized" bismuth oxides.

In order to realize the phase transformation during thermal treatment, high temperature XRD was applied to examine this behavior. Fig. 8 shows high temperature XRD patterns of calcined 7.5TSB powder by various holding times, 30 or 10 min, and heating/cooling rate, 3 °C/min or 10 °C/min before each

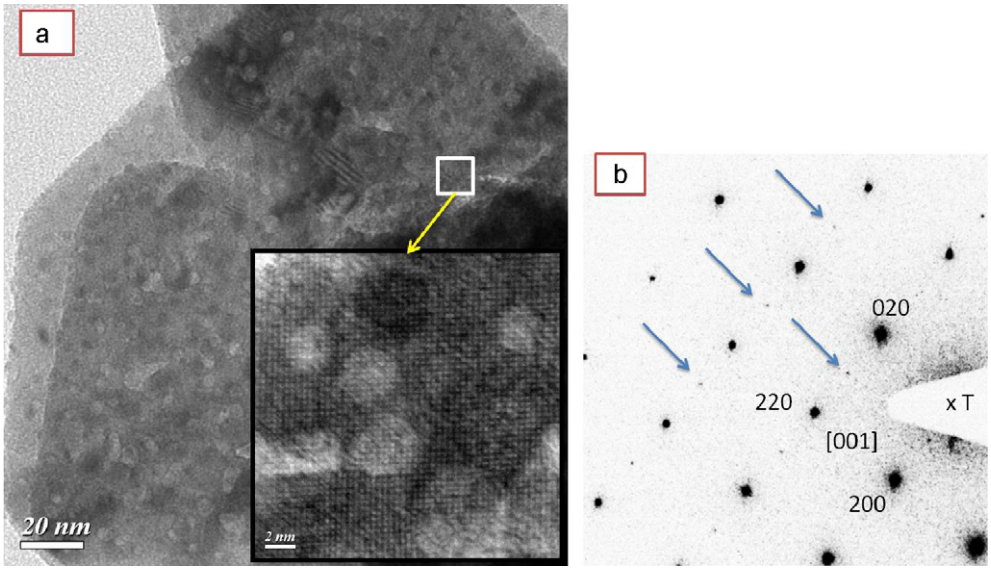

Fig. 5. (a) TEM image and (b) diffraction pattern of 7.5TSB treated at 850 °C for 1 h. The inset is a HETEM micrograph illustrating the structural details in the square in (a).

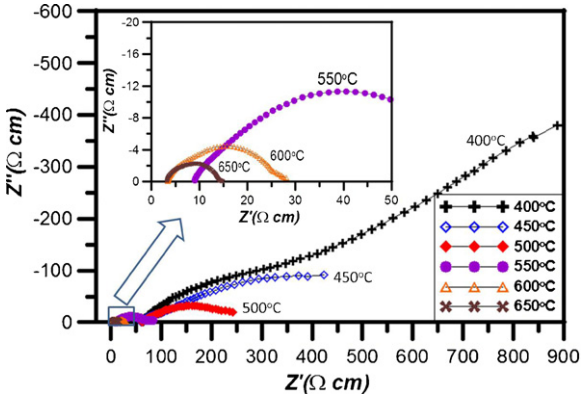

Fig. 6. Nyquist plot of 850 °C/1 h sintered 7.5TSB as a function of temperature. Heating rate is 10 °C/min, holding for 30 min before each measurement.

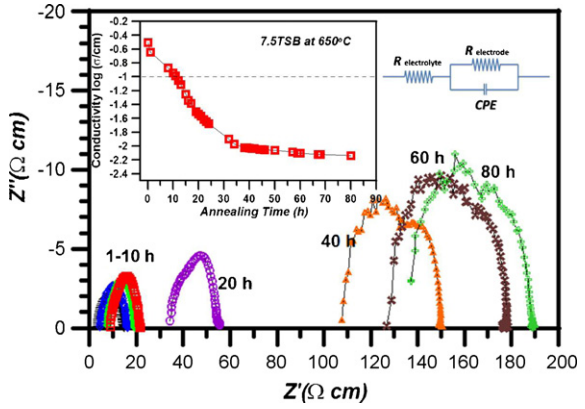

Fig. 7. Nyquist plots of 850 °C/1 h sintered 7.5TSB as a function of time tested at 650 °C up to 80 h. The inset is the conductivity, which is calculated from bulk resistance read from the Nyquist plots of this case.

measurement. The pattern show that B3T (type II) phase formed as low as 600 °C. After cooling down to 50 °C, B3T phase remained in the pattern, indicating that the formation of B3T phase is thermally non-reversible. Comparing to the case treated at 850 °C for 100 h, no B3T phase but pure type I phase was detected, which represents that type I phase of 7.5TSB is not thermodynamic stable at 700 °C and has metastable type I with other two phases, similar Er_2O_3–Bi_2O_3[16] and Bi_2O_3–Er_2O_3–PbO[20] systems.

Measurement with slower heating rate (Fig. 8(b)) shows that γ-Bi_2O_3 was found at 650 °C during heating. After cooled down to 50 °C, three phases co-existed. The results of high temperature XRD depicts that new phases at 600–750 °C may occur. Three reasons, oxygen vacancy ordering, nano-pore formation, and (B3T + γ-Bi_2O_3) phase formation, result in the conductivity degradation of 7.5TSB at 650 °C.

The effect of long-term annealing is tested. The dense 7.5TSB sample underwent 1000 h annealing at 650 °C, the stable phases were indexed as α-Bi_2O_3 (#65-2366)*[a] and type II, as shown in Fig. 9(c). This implies that the γ-Bi_2O_3 phase observed by

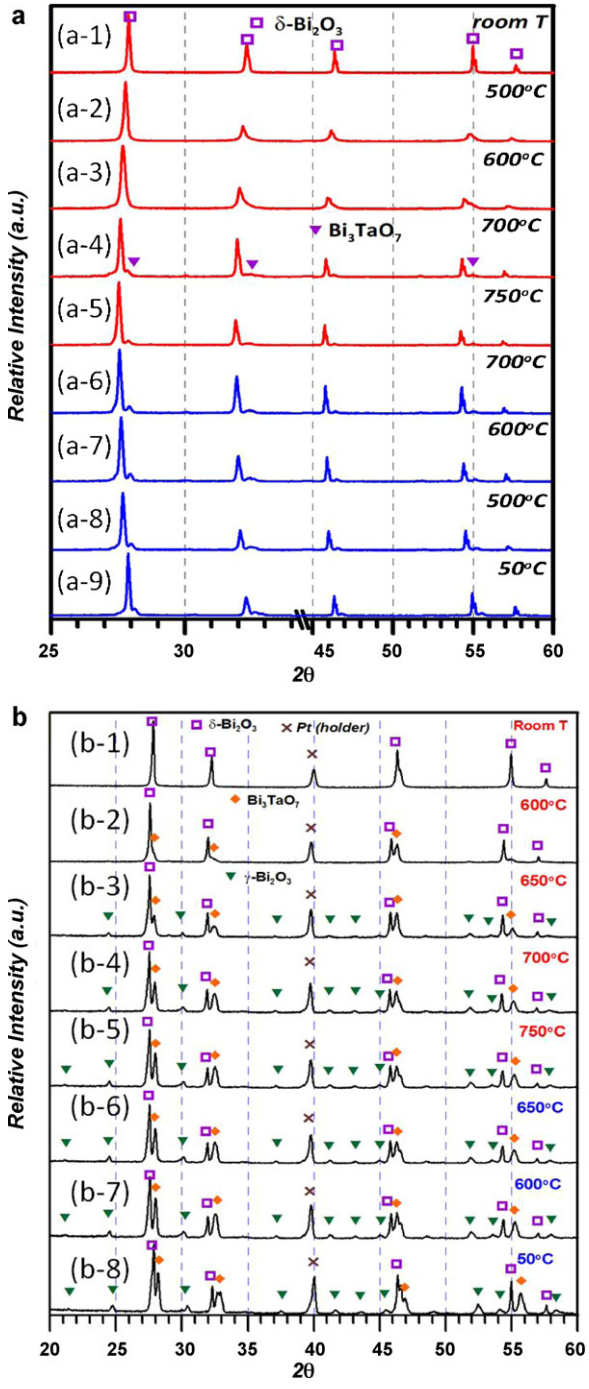

Fig. 8. High temperature XRD patterns of pre-calcination 7.5TSB (850 °C/1 h) with heating and cooling rate of (a) 10 °C/min, the test was conducted after held for 10 min at specified temperature. (b) At a heating rate of 3 °C/min, the test was conducted after held for 30 min at specified temperature. The testing samples are in powder state.

HT-XRD is not a thermodynamic stable phase, opposite to α-Bi_2O_3. Furthermore, those two phases disappeared if the sample was heated to 850 °C for 1 h again (Fig. 9(d)).

The samples of 2–7 mol% Gd_2O_3 doped Bi_2O_3[22] were cubic (δ-) phase at higher temperature (800 °C), and transformed into tetragonal β-phase during cooling. Their cases showed the samples annealing at ≤660 °C for several hundred hours, tetragonal

[a] The phase was named "Sillenite" after the founder Sillen reported in Z. Kristallogr. 103 (1940) 274–290.

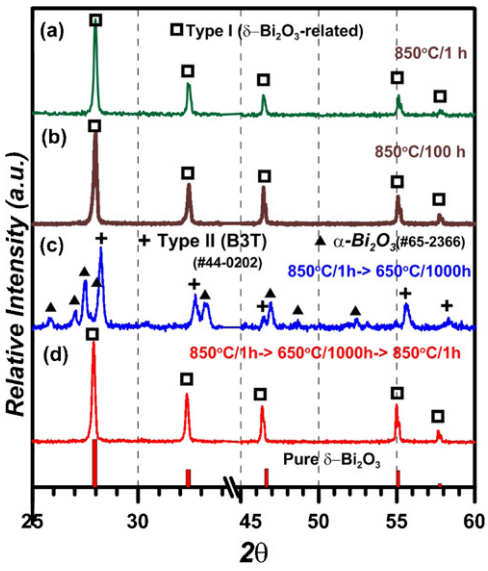

Fig. 9. XRD patterns of 7.5TSB calcined at 850 °C for (a) 1 h and (b) 100 h. (c) 1 h then annealed at 650 °C for 1000 h. (d) Re-treated at 850 °C for 1 h again.

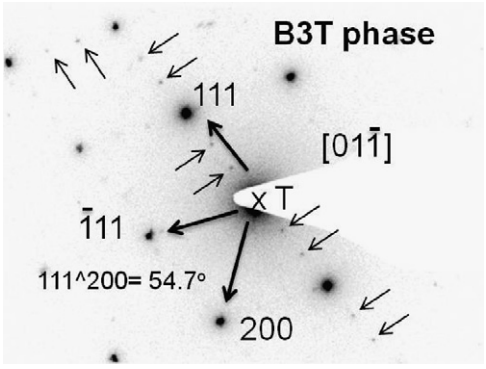

Fig. 10. Diffraction pattern of 850 °C/1 h calcined 7.5TSB annealed at 650 °C for 1000 h, indicating ⟨1 1 1⟩ vacancy ordering in structure. T means transmitted electron beam.

phase decomposes into monoclinic and rhombohedral phases, meaning tetragonal polymorph is a metastable phase. Their case is similar to the transformation of γ-Bi_2O_3/α-Bi_2O_3 phases by long-term treatment in this study.

Electron diffraction patterns of a 650 °C/1000 h annealed sample (the same as Fig. 9(c)) is shown in Fig. 10. Superlattice reflection align in ⟨1 1 1⟩ for the phase of B3T, represents the vacancy defects to be ordered in ⟨1 1 1⟩. Abrahams et al.[13] have reported the conductivity properties of type II phase, which is obvious one to two orders lower than δ-Bi_2O_3. As a result, the degradation of conductivity at 650 °C might be due to the phase separation and vacancy defect ordering in type II phase.

4. Conclusion

Bi_2O_3 samples doped with 5–10 mol% Ta_2O_3 were prepared and characterized in this study. Single-phase dense 7.5TSB can be prepared by sintering at 850 °C for 1 h and performs acceptable conductivity at 650 °C. However, the results of the sample by long-term annealing at 650 °C showed that the conductivity degraded one to two orders of magnitude, due to the phase transformation to γ-Bi_2O_3/α-Bi_2O_3 phases.

Long-term heat treatment resulted in thermally stable α-Bi_2O_3 and type II phases. However, the δ-phase can be retrieved by heating to 850 °C. Electron diffraction of type II phase revealed defect ordering in ⟨1 1 1⟩ after annealing at 650 °C for 1000 h. As a result, the degradation of conductivity at 650 °C is induced due to the phase transformation and vacancy ordering in type II phase.

References

1. Gattow G, Schröder H. Über Wismutoxide. III. Die Kristallstruktur der Hochtemperaturmodifikation von Wismut(III)-oxid (δ-Bi_2O_3). *Z Anorg Allg Chem* 1962;**318**:176–89.
2. Harwig HA, Gerards AG. The polymorphism of bismuth sesquioxide. *Thermochim Acta* 1979;**28**:121–31.
3. Sammes NM, Tompsett GA, Nafe H, Aldinger F. Bismuth based oxide electrolytes – structure and ionic conductivity. *J Eur Ceram Soc* 1999;**19**:1801–26.
4. Ling CD, Withers RL, Schmid S, Thompson JG. A review of bismuth-rich binary oxides in the systems Bi_2O_3–Nb_2O_5, Bi_2O_3–Ta_2O_5, Bi_2O_3–MoO_3, and Bi_2O_3–WO_3. *J Solid State Chem* 1998;**137**:42–61.
5. Taremechenko AA, Kharton VV, Naumovich EN, Samokhval VV. Oxygen ionic and electronic conductivity of La-doped BIMEVOX. *Solid State Ionics* 1998;**111**:227–36.
6. Suzuki T, Kaku K, Ukawa S, Dansui Y. Low-temperature performance of thin solid electrolyte cell based on MoO_3-doped Bi_2O_3. *Solid State Ionics* 1984;**13**:237–9.
7. Barreca D, Rizzi GA, Tondello E. A chemical vapour deposition route to MoO_3–Bi_2O_3 thin films. *Solid State Ionics* 1998;**333**:35–40.
8. Valant M, Suvorov D. Dielectric characteristics of bismuth oxide solid solutions with a fluoirte-like crystal structure. *J Am Ceram Soc* 2004;**87**:1056–61.
9. Tompsett GA, Sammes NM, Zhang Y, Watanabe A. Characterization of WO_3-, V_2O_5-, and P_2O_5-doped bismuth oxides by X-ray diffraction and Raman spectroscopy. *Solid State Ionics* 1998;**113**(115):631–8.
10. Zhou W. Structural chemistry and physical properties of some ternary oxide in the Bi_2O_3–Ta_2O_5 system. *J Solid State Chem* 1992;**101**:1–17.
11. Fruth V, Ianculescu A, Berger D, Preda S, Voicu G. Synthesis, structure and properties of doped Bi_2O_3. *J Eur Ceram Soc* 2006;**26**:3011–6.
12. Saito T, Miida R. Crystal structure and ionic conductivity in Bi_2O_3-rich Bi_2O_3–Ta_2O_5 sintered oxides. *Jpn J Appl Phys* 1999;**38**:4838–42.
13. Abrahams I, Krok F, Struzik M, Dygas JR. Defect structure and electrical conductivity in Bi_3TaO_7. *Solid State Ionics* 2008;**179**:1013–7.
14. Asryan NA, Kol'tsova TN, Alikhanyan AS, Nipan GD. Thermodynamics and phase diagram of the Bi_2O_3–SnO_2 system. *Inorg Mater* 2002;**38**:1141–7.
15. Miyayama M, Yanagida H. Oxygen ion conduction in fcc Bi_2O_3 doped with ZrO_2 and Y_2O_3,. *Mater Res Bull* 1986;**21**:1215–22.
16. Fung KZ, Baek HD, Virkar AV. Thermodynamic and kinetic considerations for Bi_2O_3-based electrolytes. *Solid State Ionics* 1992;**52**:199–211.
17. Mazurkevich YS, Kobasa IM. TiO_2–Bi_2O_3 materials. *Inorg Mater* 2002;**38**:522–5.
18. Weng CH, Wei WCJ. Synthesis and properties of homogeneous Nb-doped bismuth oxide. *J Am Ceram Soc* 2010;**93**:3124–9.
19. Paterson A, Stevens R. Phase analysis of sintered yttria–zirconia ceramic by X-ray diffraction. *J Mater Res* 1986;**1**:295–9.
20. Webster NAS, Ling CD, Raston CL, Kincoln FJ. The structural and conductivity evolution of fluorite-type Bi_2O_3–Er_2O_3–PbO solid electrolytes during long-term annealing. *Solid State Ionics* 2008;**179**:697–705.
21. Jiang N, Wachsman ED. Structural stability and conductivity of phase-stabilized cubic bismuth oxides. *J Am Ceram Soc* 1999;**82**:3056–7.
22. Su P, Virkar AV. Cubic-to-tetragonal displacive transformation in Gd_2O_3–Bi_2O_3 ceramics. *J Am Ceram Soc* 1993;**76**:2513–20.